

Ferromagnetic properties of potassium clusters incorporated into zeolite LTA

Yasuo Nozue, Tetsuya Kodaira, Satoshi Ohwashi, Takenari Goto, and Osamu Terasaki
Department of Physics, Faculty of Science, Tohoku University, Aramaki Aoba-ku, Sendai 980, Japan

(Received 25 March 1993)

Ferromagnetic properties are reported for K clusters incorporated into the α cage (supercage) of zeolite LTA. In LTA, α cages are arrayed in a simple cubic structure with a lattice constant of 12.3 Å. The average 4s-electron number per cluster, n , is systematically changed from 0.8 to 7.3 by controlling the K loading density. Ferromagnetism is observed for $2-3 < n < 6-7$. The magnetization shows a peak at $n \sim 5$, and the average magnetic moment amounts to $0.24\mu_B$ per cluster at 100 Oe and 1.7 K. The Curie temperature is n dependent and less than 7 K. Magnetic properties are basically interpreted in terms of the model of itinerant electron ferromagnetism. Narrow energy bands due to the electron transfer between adjacent clusters play an important role in the construction of a model. The magnetic properties exhibit spin-glass and reentrant spin-glass phenomena depending on the K loading density.

I. INTRODUCTION

Magnetism is one of the extremely important quantum-mechanical phenomena in correlated electron systems. In particular, the possible existence of a ferromagnetic or antiferromagnetic ground state in new substances has been one of the more fascinating subjects. The Hubbard Hamiltonian, due to its simplicity, allows for ease of comprehension of correlated electrons with a localized nature. Many reports have predicted a magnetic phase diagram as functions of the intersite transfer energy, the on-site Coulomb repulsion energy, and the electron occupation. Usually, control of the number of occupying electrons in a wide range is difficult in actual materials, because of the occurrence of structural phase transition.

Zeolite crystal includes well-defined cages or channels specific to its type. New material designs have been expected to exist in the zeolite space.¹ If we incorporate clusters into arrayed cages in zeolite, clusters will interact with each other through windows between cages, and macroscopic phenomena can be expected. In LTA, which is a type of zeolite, the α cage (supercage) is surrounded by eight β cages (sodalite cages).² The α cages with an inner diameter of ~ 11 Å are arrayed in a simple cubic structure with a lattice constant of 12.3 Å. They are connected by shared windows with an inner diameter of ~ 5 Å. In an ideal Na-form LTA, 12 Na⁺ ions are distributed in the space of the framework. The chemical formula is given as Na₁₂Al₁₂Si₁₂O₄₈.

The Na₄³⁺ paramagnetic cluster has been observed in the Na-form FAU, so-called NaY, from ESR measurement.³ Various kinds of alkali-metal clusters have been investigated in FAU,⁴⁻¹² SOD (sodalite),¹³⁻¹⁵ and LTA.¹² A metallic state has been elucidated by ESR measurement of FAU containing high-density alkali metal.⁵ Optical measurements have been reported for Na clusters incorporated into the Na-form FAU,³ Na-form LTA,¹⁶ and Na-form SOD,¹⁵ and for K clusters incorporated into K-form LTA.^{17,2} In Cs clusters, the temperature dependence of the ESR signal has been discussed

from the viewpoint of the intercluster electron correlation.^{10,11}

In a previous paper, we incorporated cationic K clusters into K-form LTA at the average guest K atom number of about four per cluster, and reported ferromagnetism.¹⁷ The K-density dependence of ferromagnetic properties has been reported briefly.¹⁸ In the present paper, the K-density dependence of ferromagnetic properties is reported in detail. Ferromagnetism is observed for $2-3 < n < 6-7$, where n is the average 4s electron number per cluster. Magnetic properties are interpreted in terms of the model of weak ferromagnetism of itinerant electrons. It is elucidated from optical measurement that narrow energy bands are realized in K-loaded K-form LTA due to the intercluster electron transfer between 1s or 1p molecular orbitals of the clusters.² These narrow energy bands play an important role in the ferromagnetic model. Ferromagnetism is observed under the condition of a partly filled 1p energy band. We briefly discuss the occurrence of ferromagnetism from viewpoint of the band degeneracy. The magnetic properties show spin-glass and re-entrant spin-glass phenomena.

II. EXPERIMENTAL PROCEDURES

Present powder particles of LTA were cubic with an average size of 4 μm .² Na-form LTA powder was transformed into the K form by ion exchange. According to the results of atomic absorption spectrometry (AAS), the chemical formula is given as K₁₀NaHAAl₁₂Si₁₂O₄₈.² This zeolite is abbreviated as K-LTA(1) hereafter.

The K⁺ ion positions in K-LTA dehydrated at 300 °C have been elucidated by x-ray structural analysis.^{19,20} Major K⁺ ions are located near the center of six-membered ring. The K⁺ ion position in present K-LTA(1), however, may differ slightly from their results, because of a higher dehydration temperature, 550 °C.² The position of K⁺ ions may be changed by the loading of K atoms.

The dehydrated K-LTA(1) powder was sealed in a

quartz glass tube together with a distilled K source and a small amount of helium gas for heat exchange. Potassium was successively adsorbed into zeolite cage through the vapor phase. The loading density of K was estimated from analysis of both of optical reflection spectrum and AAS.² The maximum K density was determined to be 7.3 atoms per α cage from AAS. This value means that the space of the α cage is almost filled with K atoms.

The spectrum of the reflection R plus the transmission T of a zeolite powder particle was obtained from that of the diffuse reflection r by the equation $R + T = 4r/(1+r)^2$.²

The ac magnetic susceptibility χ was measured using the Hartshorn inductance bridge. The value was calibrated with $\text{MnSO}_4 \cdot (\text{NH}_4)_2\text{SO}_4 \cdot 6\text{H}_2\text{O}$. The strength and frequency of the modulation magnetic field were ± 78 mOe and 405 Hz, respectively. The external dc magnetic field was applied parallel to the modulation field. The magnetic susceptibility of zeolite powder without guest K atoms is less than 10^{-6} emu/cm³ over the measured temperature range. The magnetization was obtained from the integration of χ with respect to the external dc magnetic field.

III. EXPERIMENTAL RESULTS

A. K-density dependence of optical reflection spectra

In Fig. 1, reflection spectra of K-loaded K-LTA(1) with various loading densities are shown by solid curves. Dotted curves indicate the region where the transmission T cannot be neglected. The loading density increases in the order of curves $a-j$, and is saturated in curve j .

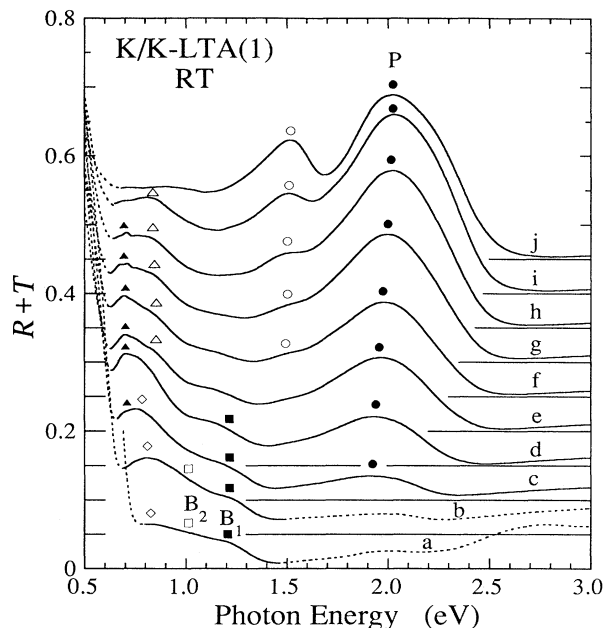


FIG. 1. Reflection spectra in K-loaded K-LTA(1) at room temperature (RT) (solid curves). The dotted curve indicates the region where the transmission component cannot be neglected. The K density increases in the order of curves $a-j$.

Hereafter, we refer to marks $a-j$ as respective sample labels. Average electron numbers per cluster are estimated to be 0.8, 1.5, 2.4, 3.2, 4.1, 4.7, 5.4, 6.0, 6.6, and 7.3 in samples $a-j$, respectively, from the reflection spectrum analysis and AAS.²

In K-loaded K-LTA, narrow energy bands are expected due to the intercluster electron transfer between $1s$, $1p$, or $1d$ molecular orbitals of K clusters in adjacent α cages. Spectra are well interpreted in terms of the optical excitation of electrons distributed in the energy bands.² In the most dilute sample a , bands B_1 and B_2 appear due to the $1s-1p$ interband transition. With increasing the loading density, bands B_1 and B_2 gradually disappear and bands between 0.7 and 0.9 eV become dominant. These bands disappear in saturated sample j . At higher loading densities, the band at 1.5 eV increases with increase in loading density. This band is assigned to the $1p-1d$ interband transition. Band P appears around 2 eV in sample c and increases to become the largest one with increase in loading density. The origin of band P is assigned to the surface plasmonlike state. The spectra in Fig. 1 indicate that $1s$ and $1p$ bands are successively occupied by $4s$ electrons with increasing K-loading density.²

An oscillator at zero frequency has been found in the reflection spectra.² This is reminiscent of the metallic state of arrayed clusters. If the Fermi energy crosses the $1s$ or $1p$ band with a finite density of state, such a Drude-like oscillator is possible at zero frequency.

In the present K cluster system, a weak potential fluctuation for electrons may be expected due to the statistical fluctuation in the distribution of guest K^+ ions. If the transfer energy between clusters is much larger than the potential fluctuation, the localized state will appear at the tail energy region of the band. As discussed in Sec. IV B, the localized state plays an important role in the expected mechanism of the spin-glass phenomenon. In the following ferromagnetic properties, however, the potential fluctuation is less important.

B. K-density dependence of ac magnetic susceptibility

The temperature dependence of ac magnetic susceptibility χ in K-loaded K-LTA(1) powder is shown in Fig. 2 in the logarithmic scale. In Fig. 3, χ is given in the linear scale. Labels $a-j$ in these figures refer to those in Fig. 1.

For reference, the calculated susceptibility of the spin $\hbar/2$ paramagnetic cluster assumed in each α cage is shown by the dotted curves in Fig. 2. If the K cluster has no interaction with adjacent ones, the susceptibility is inversely proportional to the temperature, i.e., the Curie law. The Curie constant is proportional to the number density of K cluster and $J(J+1)$, where J is the angular momentum quantum number of cluster. In the dotted curves, the number density and J are 5.3×10^{20} cm⁻³ and $\frac{1}{2}$, respectively.

In sample a in Fig. 2, χ shows the paramagnetic value given by the dotted curve below 7 K, but the temperature dependence deviates from the Curie law. Above 7 K, χ falls to a value much smaller than the dotted curve. Hence, the temperature dependence follows neither Curie law nor Curie-Weiss (CW) law. With increasing loading

density, χ at lower temperatures grows by several orders of magnitude, and shows ferromagnetic values of the order of 0.1 emu/cm^3 in samples *d* and *e*. At higher temperatures, χ decreases to values smaller than the dotted curve. In samples *e-g* in Fig. 3, χ reaches the saturation value at lower temperatures, because of a demagnetizing field. Zeolite powder particles used in the present experiment have a cubic shape. If we assume the demagnetizing factor of a spherical particle, $\frac{1}{3}$, the saturation value of χ is $3/4\pi$. Compensated susceptibility is given by $\chi/(1-4\pi\chi/3)$. The compensation is significant above $\sim 0.01 \text{ emu/cm}^3$.

With increasing loading density in Fig. 2(b), the slope at higher temperatures shifts to lower temperatures; moreover, the ferromagnetic region shifts to the lower temperature region. In samples *f-h*, χ approaches the paramagnetic value of $\lesssim 10^{-4} \text{ emu/cm}^3$ at higher tem-

peratures. In sample *i*, χ gives paramagnetic values throughout the given temperature range. In sample *j*, χ is larger than in sample *i*.

In curves *e-g* in Fig. 3, χ decreases slightly at lower temperatures. This behavior is discussed from the viewpoint of the reentrant spin-glass phenomenon in Sec. IV B. As shown later in Sec. III D, χ decreases with time by a few percent just after removal of the applied *dc* magnetic field *H* in samples *e-g*. This result is assigned to the slow dynamics of the spin-glass phenomenon, and is discussed in Sec. IV B.

The reciprocal plot of χ is given in Fig. 4 in the range $0-4 \times 10^3 \text{ cm}^3/\text{emu}$. This range is considerably smaller than that usually plotted. Labels *b-j* refer to those in the previous figures. The dotted line shows the calculated susceptibility of the spin $\hbar/2$ paramagnetic cluster assumed in each α cage; namely, each cluster is assumed to have a localized magnetic moment of $1.73\mu_B$. In samples *e-i*, the CW law seems to be satisfied. An effective mag-

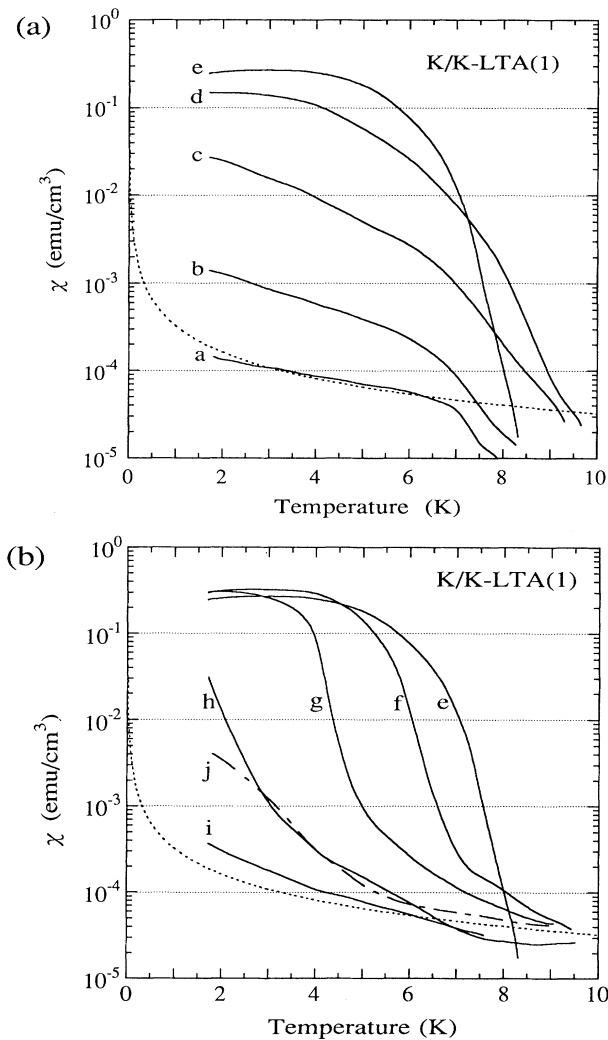


FIG. 2. Temperature dependence of ac magnetic susceptibility in K-loaded K-LTA(1) for (a) lower and (b) higher K densities. Labels *a-j* are the same as in Fig. 1. The dotted curve indicates the calculated susceptibility of spin $\hbar/2$ paramagnetic clusters assumed in each α cage.

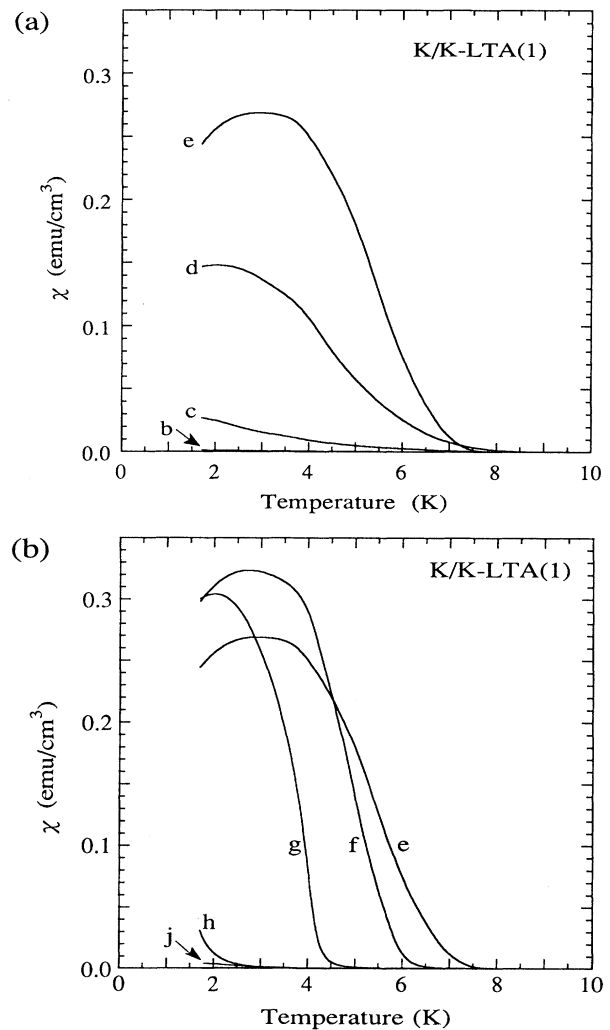


FIG. 3. Temperature dependence of ac magnetic susceptibility in K-loaded K-LTA(1) in a linear scale for (a) lower and (b) higher K densities. Labels *b-j* are same as in Figs. 1 and 2.

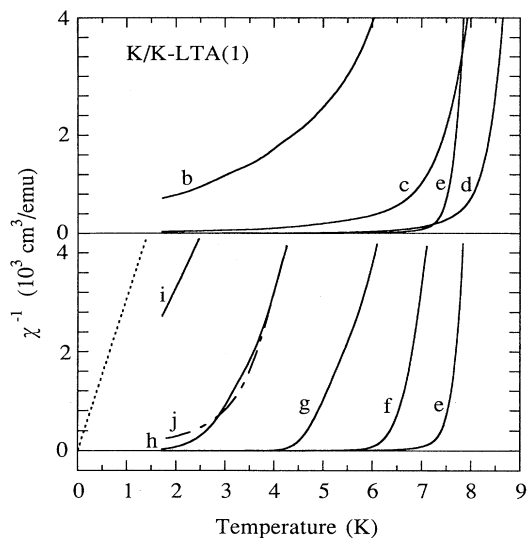


FIG. 4. Temperature dependence of the reciprocal of magnetic susceptibility in K-loaded K-LTA(1). The dotted line indicates the reciprocal of calculated susceptibility in independent magnetic moment with a localized spin $\hbar/2$ in each α cage.

netic moment is estimated to be on the order of μ_B per cluster. The curves in a wide range, however, are not simple. In sample *g*, for example, the temperature (T_s) dependence near the Curie temperature (T_c) approximates that given by the function $\chi^{-1} \propto (T_s - T_c)^2$ for $T_s > T_c$, where $T_c = 4.1$ K. This temperature dependence is expected near T_c according to the self-consistent renormalization (SCR) theory of spin fluctuations in itinerant electron ferromagnetism.^{21,22}

In other curves *b-d* and *j*, the curvature widely deviates from the CW law as well as the temperature dependence in the SCR theory. As stated later, these samples are in the spin-glass state. A deviation from the Curie-Weiss law has been observed in the spin-glass susceptibility in AuFe alloy.²³

The systematic estimation of the Curie temperatures in all samples is so difficult that we plot the temperature at which $\chi = 0.1, 0.01,$ and 0.001 emu/cm³ as a function of the average electron concentration per cluster in Fig. 5. In this figure, sample labels *b-h* and *j* are shown in the corresponding places. The maximum temperature is observed at the electron concentration of 3–4 per cluster.

C. K-density dependence of magnetization

In Fig. 6, the external dc magnetic field (H) dependence of the magnetization (M) at 1.7 K is shown for samples *b-h* and *j*. The values of M in samples *a* and *i* are negligible in this scale, and the data are not shown here. The magnetization values in samples *a, b,* and *i* are given in Fig. 7 in a fine scale. Except for sample *h*, M increases rapidly at H less than ~ 5 Oe, and gradually increases above ~ 5 Oe. In sample *h*, M continues to increase with H in the range given in the figure.

In the previous paper,¹⁷ a weak hysteresis of M with respect to H has been observed. In the present ferromag-

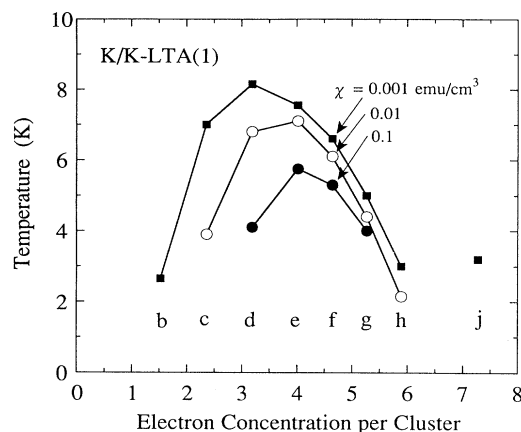


FIG. 5. Temperature at which $\chi = 0.1, 0.01,$ and 0.001 emu/cm³ as a function of the electron concentration per cluster. Sample labels *b-h* and *j* are shown in the figure.

netic samples, the hysteresis is hardly observed. A weak hysteresis is observed only in saturated sample *j*. Generally, the strength of coercive force depends on magnetic anisotropy and/or defect content. The present samples were sufficiently annealed such that the uniformity is better than that in the previous samples.

The values of χ or M in samples *a, b,* and *j* are not ferromagnetic, but are very sensitive to H . Usually, susceptibility of paramagnetic moment depends on H in the scale of 10^4 Oe at these temperatures. As discussed in Sec. IV B, the H sensitivity in samples *a, b,* and *j* is interpreted in terms of the spin-glass model: inhomogeneously distributed ferromagnetic regions show a magnetic correlation between them due to the Ruderman-Kittel-Kasuya-Yosida-like (RKKY) interaction.

The magnetization M at 100 Oe and 1.7 K is plotted in Fig. 8 as a function of the electron concentration per

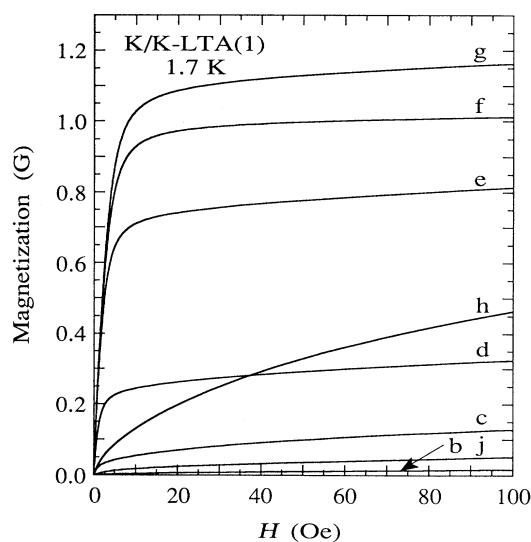


FIG. 6. Magnetic-field dependence of magnetization in K-loaded K-LTA(1). Sample labels *b-h* and *j* are shown in the figure.

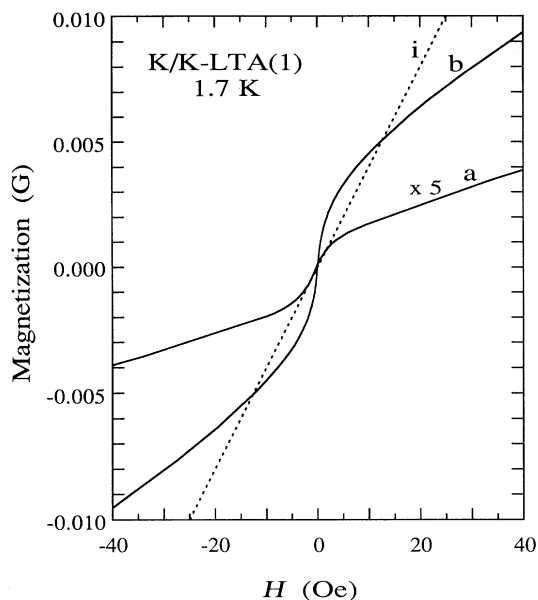


FIG. 7. Magnetic-field dependence of magnetization in samples *a*, *b*, and *i* of K-loaded K-LTA(1).

cluster. The magnetization increases above 2–3 electrons, shows a peak at ~ 5 , and a minimum at 6.6. The magnetization increases again at 7.3 electrons. The maximum value of magnetization, 1.17 G, is seen in sample *g*. This magnetization corresponds to the average magnetic moment per cluster of $0.24\mu_B$. The above result is quite analogous to the Slater-Pauling plot for the average magnetic moment of $3d$ disordered transition-metal alloys.

In the present samples, the magnetic moment estimated from magnetization is considerably smaller than that roughly estimated from the temperature dependence of χ above the Curie temperature. In itinerant electron ferromagnetism, the magnetic moment estimated from magnetization is known to be smaller than that estimated

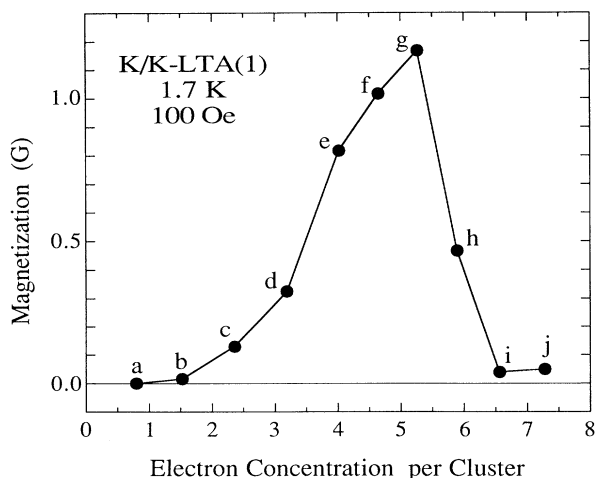


FIG. 8. Magnetization at 1.7 K and 100 Oe in K-loaded K-LTA(1) as a function of the electron concentration per cluster.

from the CW law. Hence, the present result suggests that magnetic properties are due to itinerant electron ferromagnetism.

The temperature dependence of the M - H curve for sample *g* is shown in Fig. 9. With increasing temperature, M decreases. It is impossible to interpret this result in terms of super paramagnetism because a plot of M as a function of temperature-normalized H depends significantly on the temperature. The magnetization at 15 Oe in samples *f* and *g* is plotted as a function of temperature in Fig. 10 together with the reciprocal of χ . We estimate the Curie temperature from the temperature dependences of magnetization and χ^{-1} . The Curie temperatures in samples *f* and *g* are 5.8 ± 0.3 and 4.3 ± 0.1 K, respectively.

In sample *f*, for example, χ decreases below 2.7 K in Fig. 3. This behavior is observed in the reentrant spin-glass phenomenon in *AuFe*.²⁴ However, M increases at the temperatures given in Fig. 10. Such temperature dependence of M is similar to that observed in *AuFe*.²⁵

D. Slow dynamics

The magnetic susceptibility in spin-glass materials is known to exhibit a slow change with time. The time dependence of normalized ac magnetic susceptibility $\chi(t)/\chi(t_0)$ in samples *e*–*g* is shown in Fig. 11 as a function of the time t just after the removal of an external dc magnetic field. The normalization time t_0 is ~ 0.5 s. The time dependence is significant in the lower K-density sample *e*. This phenomenon is referred to as slow dynamics. Slow dynamics has been observed in the magnetization in *AuFe*.²⁶ This phenomenon is caused by the slow reconstruction of a stable magnetic arrangement under applied magnetic field.

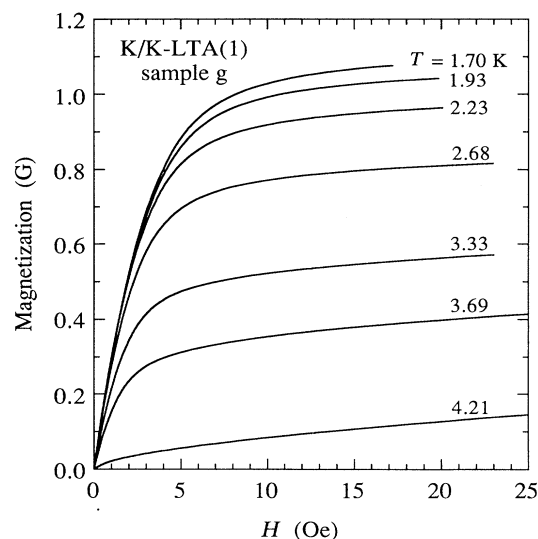


FIG. 9. Magnetic-field dependence of magnetization in sample *g* of K-loaded K-LTA(1) below the Curie temperatures.

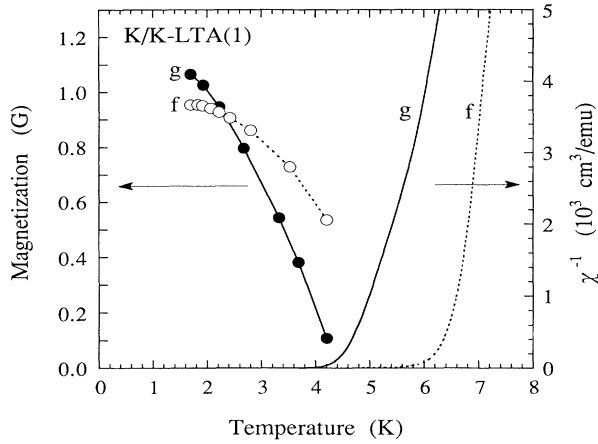


FIG. 10. Temperature dependences of magnetization and reciprocal of χ in samples *g* and *f* of K-loaded K-LTA(1).

IV. DISCUSSION

A. Ferromagnetism

Ferromagnetism is generally recognized to be the result of electron correlation. If electrons are completely localized at each cluster, they will exhibit paramagnetism and diamagnetism in open and closed shells of localized electronic states, respectively. Free-electron metals such as potassium exhibit Pauli paramagnetism and Landau diamagnetism,²⁷ but no ferromagnetism at any electron density.^{28,29} Based on the above point of view, the present K-cluster system is classified as neither a completely localized electron system nor a free electron metal, but as a system with both a localized nature and itinerancy.

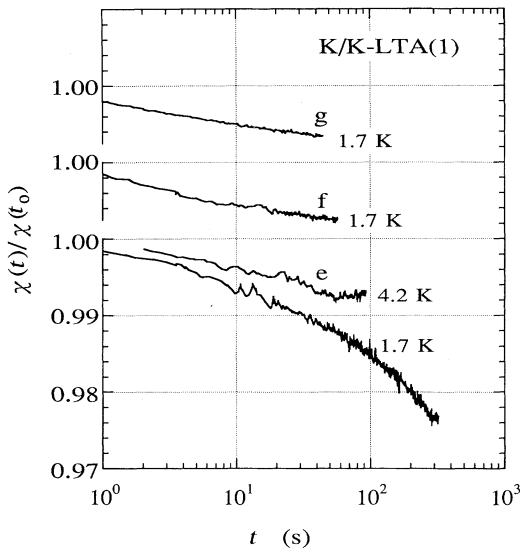


FIG. 11. Time dependence of magnetic susceptibility $\chi(t)$ in samples *e*–*g* of K-loaded K-LTA(1). Time t is measured just after the removal of the external magnetic field. $\chi(t)$ is normalized by $\chi(t_0=0.5s)$.

From the viewpoint of optical properties, it is concluded that a K cluster is generated in each α cage and that $1s$ - and $1p$ -like molecular orbitals are occupied successively by $4s$ electrons of K with increasing K density. This result can be understood within the zeolite space as follows.² Since the framework of zeolite LTA has a negative charge, the framework potential repulses electrons. Host and guest K^+ ions distributed in the space of the framework attract electrons. The average distance between adjacent K^+ ions in LTA is comparable to the effective diameter of one K atom, $\sim 5 \text{ \AA}$. Hence, the $4s$ electron of K atoms can be delocalized in the space of zeolite. Since the framework acts as a potential barrier to electrons, the potential well for electrons is realized in α and β cages. In the case of K-form LTA, doped electrons are confined only in the α cage, because the resultant energy of the localized state in the α cage is lower than that in the β cage.² The α cage has six windows with a diameter of 5 \AA , and these windows are shared with the adjacent α cage. The framework potential for electrons may be lowered at windows because of the weakness of the framework-repulsive potential. If cations are distributed near windows, the potential for electrons is lowered further. Therefore, an overlap between molecular orbitals in adjacent α cages is expected at the windows.

If we assume an ideal periodic potential for electrons in LTA, narrow energy bands originating from $1s$ and $1p$ molecular orbitals are expected according to the analogy of a tight-binding model. The energy dispersion may have a large cubic anisotropy, because electrons are transferred only through windows. As stated later in Sec. IV B, the potential disorder should be considered in a detailed analysis of experimental results, but we discuss here the occurrence of ferromagnetism in an ideal model. The disorder effect is discussed later with respect to the spin-glass phenomenon.

The ground-state magnetic phase diagram in narrow-band metals has been calculated by many researchers. If the Hubbard Hamiltonian is calculated according to the Hartree-Fock and random-phase approximations, we obtain a result equivalent to the Stoner model. According to the Stoner model, the ferromagnetic state at 0 K occurs under the Stoner condition

$$\frac{U\rho(E_f)}{N} > 1, \quad (1)$$

where U is the Coulomb repulsive energy between two electrons in the same cluster (site), $\rho(E_f)$ is the density of state at the Fermi energy E_f , and N is the number density of clusters (sites). The Stoner model, however, leads to quite insufficient results at finite temperatures. An SCR theory of coupled modes of extended spin fluctuations has been successfully applied for the improvement of the theory.^{21,22}

Equation (1) seems to be easily satisfied in any narrow energy band. The electron correlation in the narrow band, however, is known to reduce U to the order of the bandwidth W , when U is much larger than W .³⁰ In this sense, U should be replaced by the effective energy U_{eff} . According to this calculation, no ferromagnetic condition can be satisfied easily in a simple band structure.³⁰ How-

ever, it is concluded from the present experimental results that the ferromagnetic K-cluster system in LTA satisfies the condition for the $1p$ energy band

$$\frac{U_{\text{eff}}\rho(E_f)}{N} > 1. \quad (2)$$

This situation is shown schematically in Fig. 12. The state densities of $1s$ and $1p$ bands are drawn for up- and down-spin electrons. If the Fermi level is located at the energy of a sufficiently high density of state, a finite population difference between up and down spins will reduce the total energy, which leads to the ferromagnetic ground state of itinerant electrons. The increase and decrease in magnetization shown in Fig. 8 may be interpreted in terms of the increase and decrease in $\rho(E_f)$ in the $1p$ band, respectively.

The temperature dependence of χ in sample i in Fig. 2 shows a CW lawlike behavior, but the expected Curie temperature is less than 0.5 K. In the SCR theory, a CW lawlike behavior is expected even when the system is critically unstable with respect to ferromagnetism.^{21,22} Hence, the observed dependence of χ may be interpreted in terms of the SCR theory for a slightly ferromagnetic system.

Blazey *et al.*¹⁰ and Blatter, Blazey, and Portis¹¹ have observed the CW law in the temperature dependence of the ESR signal in Cs clusters incorporated into zeolite FAU. They have found a negative Curie temperature in Cs-rich clusters, and expected an antiferromagnetic correlation between clusters. However, they found no evidence of the Néel point. Hence, antiferromagnetism is not conclusive. The ESR spectrum of the clusters is metallic. Their temperature dependence can be interpreted in terms of the CW lawlike behavior given in the SCR theory of a metallic system in which the ferromagnetic condition is not completely satisfied. A similar result ob-

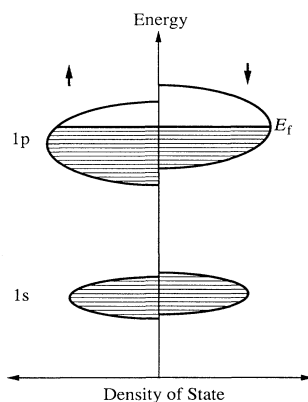


FIG. 12. Schematic representation of the model of the itinerant electron ferromagnetism in K-loaded K-LTA(1). The density of state is shown for up- and down-spin electrons in energy bands originating from $1s$ and $1p$ molecular orbitals of the K cluster. If the Fermi energy E_f is located at the energy of a sufficiently high state density for the $1p$ band, a finite population difference between up and down spins minimizes the total energy, resulting in ferromagnetism.

served in Na clusters in FAU (Ref. 12) may be also interpreted using the same model. The Curie law observed in the ESR signal of K clusters incorporated into FAU (Refs. 8, 10, and 11) at higher K densities can be interpreted with the similar model of the system, but in the critical condition of ferromagnetism.

The ferromagnetic instability of itinerant electrons has been calculated according to various methods based on the Hubbard model. In the strong correlation limit $U = \infty$, a ferromagnetic state (Nagaoka state) in the one-band Hubbard model has been calculated in the thermodynamic limit.³¹ The stability of the Nagaoka state has been investigated by many researchers.³² Recently, ferromagnetism has been found in the degenerate single-electron ground state.³³ Variational methods, such as Gutzwiller's method, have been adopted in order to clarify the magnetic phase diagram.^{34,35} Aside from these, itinerant electron magnetism in the nondegenerated energy band has been investigated by means of a self-consistent moment method,³⁶ fourth-order perturbation expansion,³⁷ and Monte Carlo simulations.³⁸

In the model given in Fig. 12, the ferromagnetic condition of Eq. (2) can be easily satisfied at the $1s$ band as well as the $1p$ band. No ferromagnetic enhancement, however, is found at the $1s$ band in Fig. 8. The on-site Coulomb energy of the $1s$ orbital is not so different from that of the $1p$ orbital, but there is an essential difference in the band degeneracy. In the case of the degenerate band, an intrasite exchange interaction, namely Hund's coupling, has been expected to play an important role in the stability of the ferromagnetic state.^{35,39} In the present system, the degeneracy of the $1p$ band may play an essential role in the stability of the ferromagnetic phase.

In the Hubbard model, the antiferromagnetic ground state may appear at the just half-filled condition, even when Hund's coupling is significant. In the present experimental result, however, no antiferromagnetic behavior appears at the just half-filled condition of the $1p$ band, i.e., five electrons per cluster. Resultant properties may be interpreted qualitatively with the model similar to that for the Slater-Pauling curves in disordered alloys of $3d$ transition metals.⁴⁰ For detailed discussion, we must obtain microscopic insight into intercluster interaction.

Here, we roughly estimate relevant parameters appearing in the Hubbard Hamiltonian for reference. We simplify the cluster potential as having an infinite barrier, a spherical shape, and an inner diameter of 11 Å. The kinetic energies of electrons in $1s$ and $1p$ orbitals are calculated to be 1.2 and 2.5 eV, respectively. On-site Coulomb repulsion energies are roughly estimated as follows by neglecting the screening effect. The Coulomb energy between two electrons in the $1s$ orbital is 4.7 eV, and that in same $1p$ orbital, 4.4 eV. The Coulomb energies between electrons in different $1p$ orbitals with singlet and triplet spin configurations are 4.1 and 3.5 eV, respectively. Hence, Hund's coupling energy is 0.6 eV. The transfer energy between adjacent clusters may be on the order of 0.1 eV according to the optical spectra.

In Fig. 8, lower K-density samples a and b exhibit slight magnetization. With increasing K density, the magnetization increases again in sample j . These magne-

tizations are ascribed to the spin glass contribution from the $1p$ and $1d$ band tails, as discussed in Sec. IV B.

B. Spin-glass and reentrant spin-glass phenomena

The spin-glass phenomenon is observed frequently in magnetically inhomogeneous materials, such as alloy containing dilute transition metal. The reentrant spin glass phenomenon has been observed in materials containing a dense magnetic element. One typical behavior in the spin-glass phenomenon is the appearance of a cusp in the temperature dependence of ac magnetic susceptibility.²⁴ The shape of the cusp is very sensitive to the amplitude of modulation magnetic field. In the reentrant spin glass phenomenon, ac magnetic susceptibility decreases below the ferromagnetic temperature.⁴¹

As shown in Sec. III C, the magnetization in lower K-density samples $a-c$ is very sensitive to the external magnetic field, but the value of χ is not ferromagnetic. The temperature dependence of χ in these samples shows no cusp in the measured temperature, but the magnetic properties can be interpreted qualitatively in terms of the spin glass phenomenon, because of the magnetic properties mentioned in Sec. III B.

Finally, we speculate on the origin of the present spin-glass phenomenon. In the electronic system having potential fluctuation, the localized state of electron appears in the upper and lower tail regions of the energy band, because of the Anderson localization. In the present K cluster system, there exists a weak potential disorder for electrons, as discussed in Sec. III A. In the localized state, an electron moves coherently over several K clusters, but has no long-range coherence. In the extended state, an electron has a relatively long-range coherence.

When E_f is located in the $1s$ band region, the localized state of the $1p$ band are occupied by electrons below E_f . A part of shallow localized states may be partly occupied by electrons, because of the repulsive interaction between electrons. Here, we assume that electrons in some localized states may have a ferromagnetic correlation giving a finite magnetic moment. These localized states are thought to be small ferromagnetic regions constructed of several K clusters. Hence, at lower K densities, small ferromagnetic regions due to the localized state of the $1p$ band are expected to be distributed sparsely in the major paramagnetic region due to the extended state of the $1s$ band. If these ferromagnetic regions interact with each other through electrons in the paramagnetic region, which is somewhat similar to the RKKY interaction, the

long-range magnetic correlation between them can be expected. This will result in the spin-glass phenomenon. With increasing the K density, the size and/or the number of ferromagnetic region will increase. Hence, the susceptibility may increase significantly, as observed in the experiments. The rapid decrease of χ above 7 K in samples a and b in Fig. 2 may be caused by the paramagnetic-ferromagnetic phase transition of these small regions.

In higher K-density samples $d-g$, E_f is located in the extended state region of the $1p$ band. The major phase may satisfy the Stoner condition, and may become ferromagnetic below the Curie temperature. The paramagnetic regions may be disturbed in the ferromagnetic region due to the potential disorder. Hence, the resultant ferromagnetic properties may show a reentrant spin-glass phenomenon at lower temperatures.

In samples h and i , the spin-glass phenomenon is not observed. This result may be interpreted with the following hypothesis. When E_f is located at the energy of extended state of the $1p$ band, the upper localized states of the $1p$ band are empty of electrons. If lower localized states are fully occupied by electrons in this condition, they have no magnetic moment. Hence, the resultant magnetic properties seem to approximate those in homogeneous materials. In sample j , small ferromagnetic regions due to the $1d$ band may be distributed in the paramagnetic phase. The above interpretations, however, are so speculative that they should be confirmed in future investigations.

V. SUMMARY

K clusters incorporated into K-LTA exhibit ferromagnetism at $2-3 < n < 6-7$, where n is the average electron concentration per cluster. This result is interpreted in terms of the model of itinerant electron ferromagnetism in the $1p$ energy band. Magnetic properties show spin-glass and re-entrant spin-glass phenomena depending on the K-loading density.

ACKNOWLEDGMENTS

This work was partly supported by a Research Grant from the Kurata Foundation and a Grant-in-Aid for Scientific Research from the Ministry of Education, Science and Culture of Japan. O.T. thanks Tosoh Corporation for support.

¹V. N. Bogomolov, Usp. Fiz. Nauk **124**, 171 (1978) [Sov. Phys. Usp. **21**, 77 (1978)].

²T. Kodaira, Y. Nozue, S. Ohwashi, T. Goto, and O. Terasaki, Phys. Rev. B **48**, 12 245 (1993).

³P. H. Kasai, J. Chem. Phys. **43**, 3322 (1965).

⁴J. A. Rabo, C. L. Angell, P. H. Kasai, and V. Schomaker, Disc. Faraday Soc. **41**, 328 (1966).

⁵M. R. Harrison, P. P. Edwards, J. Klinowski, and J. W. Tho-

mas, J. Solid State Chem. **54**, 330 (1984).

⁶P. P. Edwards, M. R. Harrison, J. Klinowski, S. Ramdas, J. M. Thomas, D. C. Johnson, and C. J. Page, J. Chem. Soc. Chem. Commun. **1984**, 982.

⁷N. H. Heo and K. Seff, J. Chem. Soc. Chem. Commun. **1987**, 1255.

⁸Y. Katayama, K. Maruyama, and H. Endo, J. Non-Cryst. Solids, **117**, 485 (1990).

- ⁹B. Xu, X. Chen, and L. Kevan, *J. Chem. Soc. Faraday Trans.* **87**, 3157 (1991).
- ¹⁰K. W. Blazey, K. A. Müller, F. Blatter, and E. Schumacher, *Europhys.* **4**, 857 (1987).
- ¹¹F. Blatter, K. W. Blazey, and A. M. Portis, *Phys. Rev. B* **44**, 2800 (1991).
- ¹²P. A. Anderson and P. P. Edwards, *J. Am. Chem. Soc.* **114**, 10 608 (1992).
- ¹³R. M. Barrer and J. F. Cole, *J. Phys. Chem. Solids* **29**, 1755 (1968).
- ¹⁴K. Haug, V. Srdanov, G. Stucky, and H. Metiu, *J. Chem. Phys.* **96**, 3495 (1992).
- ¹⁵V. I. Srdanov, K. Haug, H. Metiu, and G. D. Stucky, *J. Phys. Chem.* **96**, 9039 (1992).
- ¹⁶T. Kodaira, Y. Nozue, and T. Goto, *Mol. Cryst. Liq. Cryst.* **218**, 55 (1992).
- ¹⁷Y. Nozue, T. Kodaira, and T. Goto, *Phys. Rev. Lett.* **68**, 3789 (1992).
- ¹⁸Y. Nozue, T. Kodaira, S. Ohwashi, and O. Terasaki, in *Proceedings of the 2nd Russian-Japan Meeting on Material Design Using Zeolite Space, St. Petersburg, 1992*, edited by V. P. Petranovskii and V. V. Poborchii (A. F. Ioffe Physical Technical Institute, St. Petersburg, Russia, 1992), p. 17.
- ¹⁹P. C. W. Leung, K. B. Kunz, K. Seff, and I. E. Maxwell, *J. Phys. Chem.* **79**, 2157 (1975).
- ²⁰J. J. Pluth and J. V. Smith, *J. Phys. Chem.* **83**, 741 (1979).
- ²¹T. Moriya and A. Kawabata, *J. Phys. Soc. Jpn.* **34**, 639 (1973); **35**, 669 (1973).
- ²²T. Moriya, *Spin Fluctuations in Itinerant Electron Magnetism*, Springer Series in Solid-State Sciences Vol. 56 (Springer-Verlag, Berlin, 1985).
- ²³A. F. J. Morgownik and J. A. Mydosh, *Solid State Commun.* **47**, 321 (1983).
- ²⁴V. Cannella and J. A. Mydosh, *Phys. Rev. B* **6**, 4220 (1972).
- ²⁵I. A. Campbell, S. Senoussi, F. Varret, J. Teillet, and A. Hamzic, *Phys. Rev. Lett.* **50**, 1615 (1983).
- ²⁶C. N. Guy, *J. Phys. F* **5**, L242 (1975); **7**, 1505 (1977); **8**, 1309 (1978).
- ²⁷Y. Takahashi and M. Shimizu, *J. Phys. Soc. Jpn.* **31**, 1612 (1971).
- ²⁸D. Pines, *Phys. Rev.* **95**, 1090 (1954).
- ²⁹K. A. Brueckner and K. Sawada, *Phys. Rev.* **112**, 328 (1958).
- ³⁰J. Kanamori, *Prog. Theor. Phys.* **30**, 275 (1963).
- ³¹Y. Nagaoka, *Phys. Rev.* **147**, 392 (1966).
- ³²B. S. Shastry, H. R. Krishnamurthy, and P. W. Anderson, *Phys. Rev. B* **41**, 2375 (1990); A. G. Basile and V. Elser, *ibid.* **41**, 4842 (1990); S. A. Trugman, *ibid.* **42**, 6612 (1990); A. M. Oles and P. Prelovsek, *ibid.* **43**, 13 348 (1991); G. S. Tian, *ibid.* **44**, 4444 (1991); J. C. Angles d'Auriac, B. Doucot, and R. Rammal, *J. Phys. Condens. Matter* **3**, 3973 (1991); D. Poilblanc, *Phys. Rev. B* **45**, 10 775 (1992).
- ³³E. H. Lieb, *Phys. Rev. Lett.* **62**, 1201 (1989); A. Mielke, *J. Phys. A* **24**, 3311 (1991); H. Tasaki, *Phys. Rev. Lett.* **69**, 1608 (1992).
- ³⁴T. Ogawa, K. Kanda, and T. Matsubara, *Prog. Theor. Phys.* **53**, 614 (1975); F. Takano and M. Uchinami, *ibid.* **53**, 1267 (1975); H. Takana and A. Okiji, *J. Phys. Soc. Jpn.* **50**, 2891 (1981); K. Hashimoto, *Phys. Rev. B* **31**, 7368 (1985); H. Yokoyama and H. Shiba, *J. Phys. Soc. Jpn.* **56**, 3570 (1987); P. Fazekas, B. Menge, and E. Müller-Hartmann, *Z. Phys. B* **78**, 69 (1990); W. von der Linden and D. M. Edwards, *J. Phys. Condens. Matter* **3**, 4917 (1991).
- ³⁵Y. Takehashi, *Phys. Rev. B* **38**, 6928 (1988).
- ³⁶W. Nolting and W. Borgiel, *Phys. Rev. B* **39**, 6962 (1989); S. Bei der Kellen, W. Nolting, and G. Borstel, *ibid.* **42**, 447 (1990); W. Nolting, S. Bei der Kellen, and G. Borstel, *ibid.* **43**, 1117 (1991).
- ³⁷B. H. Zhao, H. Q. Nie, K. Y. Zhang, K. A. Chao, and R. Micnas, *Phys. Rev. B* **36**, 2321 (1987).
- ³⁸J. E. Hirsch, *Phys. Rev. B* **35**, 1851 (1987).
- ³⁹J. H. Van Vleck, *Rev. Mod. Phys.* **25**, 220 (1953); L. M. Roth, *Phys. Rev.* **149**, 306 (1966); F. Brouers and F. Ducastelle, *J. Phys. (Paris)* **36**, 851 (1975); C. Lacroix-Lyon-Caen and M. Cyrot, *J. Phys. C* **9**, 3789 (1976); C. Lacroix-Lyon-Caen and M. Cyrot, *Solid State Commun.* **21**, 837 (1977); A. M. Oles, *Phys. Rev. B* **23**, 271 (1981); M. Tada and K. Kubo, *Prog. Theor. Phys.* **72**, 15 (1984); K. Kubo, *J. Phys. Soc. Jpn.* **51**, 782 (1982); A. M. Oles, *Phys. Rev. B* **28**, 327 (1983); A. M. Oles and G. Stolhoff, *ibid.* **29**, 314 (1984); C. Lacroix, *ibid.* **29**, 2825 (1984); W. Gill and J. Scalapino, *ibid.* **35**, 215 (1987); K. Kusakabe and H. Aoki, *J. Phys. Soc. Jpn.* **61**, 1165 (1992).
- ⁴⁰Y. Takehashi, *Prog. Theor. Phys. Suppl.* **101**, 105 (1990).
- ⁴¹B. R. Coles, B. V. B. Sarkissian, and R. H. Taylor, *Philos. Mag. B* **37**, 489 (1978).